Generation Maintenance Scheduling Based on the Remaining Useful Life of Thermal Units Considering Uncertainties via Robust Optimization Approach

Mahdi Ramezani[1], Amir Abdollahi[1,*], Masoud Rashidinejad[1], and Ali Riki[1]

[1] *Department of Electrical Engineering, Shahid Bahonar University of Kerman, Kerman, Iran*
**Corresponding author: a.abdollahi@uk.ac.ir*

Manuscript received 05 August, 2025; revised 05 September, 2025; accepted 10 September, 2025. Paper no. JEMT-2507-1566.

The efficient and reliable operation of power systems is of critical importance, as unplanned outages resulting from unit failures can cause substantial financial losses, disrupt electricity supply, and compromise grid stability. Maintenance plays a pivotal role in ensuring operational continuity. Traditionally, Generation Maintenance Schedules (GMS) have been either time-based or reactive, which can result in premature servicing or unexpected equipment failures. The prediction of Remaining Useful Life (RUL) addresses these limitations by enabling a more precise estimation of when a component is likely to fail. This paper proposes a comprehensive framework for GMS based on RUL. The degradation states and remaining operational lifespans of thermal units are estimated using a deep learning approach based on Long Short-Term Memory (LSTM) networks. Additionally, a Robust Optimization (RO) method is employed to account for uncertainties in electrical load demand and renewable energy generation. Simulation results demonstrate that the proposed RUL-based GMS framework achieves a 2.41% reduction in total system operation and maintenance costs, highlighting its effectiveness in improving system reliability and cost efficiency.

Keywords: *Generation maintenance scheduling, LSTM network, Robust optimization approach, RUL prediction.*

http://dx.doi.org/10.22109/jemt.2025.537399.1566

Nomenclature

Sets and indexes

i	Units index
N	Set of generation units (26 units)
t	Time index [week]
T	Set of time (52 weeks)

Parameters

α_i , b_i , c_i	Quadratic, linear and constant coefficient of units
h_i	RULs factor
L_t	Total demand in week t [KW]
P_i^{Min} , P_i^{Max}	Minimum a maximum power output of generation unit i [KW]
P_t^{PV}	PVs generation in week t [KW]
γ_i	Cost of rebuilding the generation unit [M$]
ζ_t , Γ_t	Uncertainty adjustment factor and uncertainty budget at week t

Variables

$b_i^{f\,/in/c/o}$	Bias vector of the forget gate/ input gate/ old cell memory/ Output gate in LSTM cell
C	Old cell memories in LSTM
$f_{t,n}$	Forget gate in LSTM cell
$IM_{i,t}$	A maintenance strategy of generating unit i in week-t (unit on maintenance = 1, otherwise = 0)
$in_{t,n}$	Input gate in LSTM cell
$\tilde{L_t}$, $\tilde{P_t^{PV}}$	Load and PV output bounded variable at week t [KW]
$\overleftarrow{L_t}$, $\overleftarrow{P_t^{PV}}$	Electrical load demand and PV output lower bounds at week t [KW]
$\vec{L_t}$, $\vec{P_t^{PV}}$	Electrical load demand and PV output upper bounds at week t [KW]
$MBPC_{i,t}$	Maintenance breach penalty cost [$]

$O_{t,n}$	Output gate in LSTM cell
$OC_{i,t}$	Operation cost of units' generation [$]
$P_{i,t}$	Generation quantity allocated to generating unit i [KW]
P_t^{UF}	Uncertainty factor [KW]
P_t^{DU}	Dual uncertainty factor [KW]
$q_{i,t}$	A binary auxiliary variable
$\vec{r}_t^{L}$, $\vec{r}_t^{L}$, $\vec{r}_t^{PV}$, $\vec{r}_t^{PV}$	Scaled deviation for load demand and Outputs at week t
$RUL_{i,t}$	Remaining useful life of unit i at week t
S	New cell memories in LSTM
$U_{i,t}$	Commitment status of generation units
$U_{n,j}^{f/in/c/o}$	Input weight matrix for forget gate/ input gate/ old cell memory / output gate in LSTM cell
$W_{n,j}^{f/in/c/o}$	Regression weight matrix for forget gate/ input gate/ old cell memory / output gate in LSTM cell
$Z_{i,t}$	Maintenance status of each unit
ΔL_t , ΔP_t^{PV}	Uncertainty bounded value of electrical load and PV at week t
ω_i	Duration of maintenance for generation [Week]
$\varpi_{i,t}$	Initiation of maintenance (maintenance begins at the start of time period=1, otherwise=0)
$\vec{\lambda}_t^{L}$, $\vec{\lambda}_t^{L}$, $\vec{\lambda}_t^{PV}$, $\vec{\lambda}_t^{PV}$	Load demand and PV output dual variable at week t

1. Introduction

1.1. Motivation and Background

Owing to economic expansion, there has been a corresponding rise in electricity demand. If this growing demand isn't matched by an equivalent expansion in generation capacity, the power system experiences reduced reserve margins. With lower reserves, utility companies often hesitate to take generators offline for maintenance, as available supply barely meets demand. As a result, insufficient maintenance leads to a higher likelihood of generator failures [1]. In recent years, South Africa has faced significant electricity generation shortages, resulting in widespread load shedding. A primary contributing factor has been inadequate maintenance, which has led to frequent boiler tube failures and subsequent plant breakdowns [2]. Due to this severe capacity deficit, the national power utility, Eskom, was compelled to implement Stage 4 load shedding, requiring the deliberate reduction of up to 4000 MW of national electricity demand at the time [3]. The GMS model outlines a timeline for preventive maintenance outages of selected generation units within a power market, while considering the constraints of the power network [4]. Optimizing the maintenance scheduling process can prolong equipment lifespan and should be prioritized to mitigate potential capital expenditures. Since modern power plants operate with high-capacity units, any outage can lead to substantial generation losses. Additionally, corrective maintenance tends to be highly expensive. Therefore, a well-structured preventive maintenance plan enhances the reliability of the power system and contributes to significant cost savings [5].

1.2. Literature review

As previously mentioned, the primary challenge addressed by the GMS model is the development of a preventive maintenance timeline for a specified set of generation units over a defined planning horizon, ensuring that all operational constraints are satisfied while meeting a designated objective function. The objectives in GMS problems are typically formulated based on either economic cost considerations or system reliability criteria.

The reliability-oriented GMS problem is commonly addressed by minimizing the Sum of Squares of the Reserve (SSR) across the entire operational planning horizon. A recent study developed a bi-objective model integrating energy hub scheduling with preventive maintenance, accounting for random equipment failures and demand uncertainty. Using a two-stage stochastic programming approach and solved via the ε-constraint method in GAMS, the model aims to minimize costs and maximize reliability [6]. A study on a practical microgrid in Lake Saroma, Hokkaido, Japan, investigated the integration of a stream tidal turbine to solve a bi-objective economic/environmental optimization problem. A Modified Multi-Objective Bird Mating Optimizer (MMOBMO) was proposed, incorporating a detailed storage cost model. Results showed improved system reliability and performance compared to the original BMO and PSO algorithms [7]. In [8] a domain-informed Deep Q-Network (DQN) framework has developed to address maintenance scheduling challenges in large-scale offshore wind farms under wake effects and weather variability. By modeling the scheduling problem as a Markov Decision Process and incorporating multiple wake models, the approach optimizes task selection and resource allocation. In [9] the GMS by incorporating environmental concerns alongside traditional reliability and cost objectives is addressed. A multi-objective GMS model is proposed to minimize operation, maintenance, and emission costs using lexicographic optimization. Additionally, a demand response program (DRP) is integrated to reduce emissions and operational expenses. The model accounts for generation unit failure probabilities and system reliability, validated through numerical tests on the IEEE 24-bus system.

The economic objective function aims to minimize the total production cost throughout the planning horizon. In [10] the complex maintenance planning and production scheduling (MPPS) problem is addressed in serial-parallel manufacturing systems under TOU tariffs. An energy-efficient two-stage maintenance (ETM) strategy is proposed to minimize total electricity and tardiness costs. The first stage optimizes preventive maintenance intervals considering machine availability, costs, and electricity price impact, while the second stage applies a mixed-integer programming model for hybrid flow shop scheduling with maintenance actions. Authors in [11] presents a mid/long-term GMS model with hourly resolution, addressing the computational challenges of large-scale integer variables. An efficient solution method combining unit clustering and linear relaxation is proposed. Starting from a Unit Commitment (UC) model, the authors develop a Relaxed Clustered Unit Commitment (RCUC) model that integrates hydropower, energy storage, pumped storage, wind, and photovoltaic plants. In [12] an integrated maintenance scheduling (IMS) strategy is developed for energy systems, considering generating units, transmission networks, power flow constraints, and renewable generation uncertainty using a scenario-based model. Energy storage is incorporated to reduce energy not supplied (ENS) during peak loads and outages. A PV power plant maintenance routing problem has been addressed in [13] that minimizes total costs, including travel, technician, downtime, and penalties, while

accounting for time-varying output due to solar radiation and temperature changes. A mixed-integer linear programming model is developed using linearization techniques, and a heuristic algorithm based on adaptive large neighborhood search is proposed for large-scale cases. Authors in [14] investigates capacity withholding (CW) through strategic maintenance in oligopoly electricity markets by proposing a security-constrained GMS model. Two indices—the relative welfare loss index and the wealth transfer index—are introduced to assess CW impacts from both nodal and global perspectives. These indices help quantify social welfare loss and wealth transfer due to strategic behavior by GenCos.

Prognostics and health management (PHM) technology plays a crucial role in maintaining the safety and reliability of power systems. As key aspects of PHM, fault diagnosis and prognosis help improve the performance and lifespan of critical components like transformers, generators, and transmission networks. A vital function of PHM is estimating the RUL, which supports proactive maintenance and accident prevention. Precise RUL prediction enables optimized maintenance planning, reduces downtime and costs, and strengthens predictive maintenance strategies, ultimately boosting power system efficiency and reliability. According to Salunkhe [15], the RUL represents the duration remaining before a failure is expected to occur. RUL—also referred to as remaining service life or remnant life—denotes the estimated time until failure, based on the current age, operational condition, and historical usage profile of the equipment. Similarly, Okoh et al. [16] define RUL as the period during which a component is still capable of fulfilling its intended function prior to failure. Approaches for predicting RUL can be categorized in various ways, depending either on the nature of the available data and system knowledge or on the methodologies and algorithms employed. Traditionally, RUL prediction methods have been broadly classified into three categories: model-based (or physics-based), data-driven, and hybrid approaches [17]. In [18] a bidirectional gated recurrent unit (BiGRU) approach combined with the bootstrap method is proposed for RUL prediction, addressing both point estimation and uncertainty quantification. The proposed method provides both RUL estimates and confidence intervals (CIs), enhancing reliability in predictive maintenance. Authors in [19] proposed a hybrid RUL prediction method that integrates model-based and data-driven approaches to improve accuracy and uncertainty quantification under small-sample conditions. The framework combines a double-exponential degradation model (DEDM) to capture degradation trends with a GRU network to predict fluctuations, while ensemble learning with a Bayesian neural network provides uncertainty quantification. In [20] the development of machine learning (ML) approaches for predicting the RUL of lithium-ion batteries is reviewed based on analysis of 380 papers over the past decade. It identifies the ten most commonly used ML algorithms, outlines key signal pre-processing techniques, and compares algorithm performance. In [21] a novel RUL prediction method is introduced that integrates expert knowledge with deep learning. Sensor relationships are encoded as flow charts, embedded, clustered, and used to guide data arrangement and model construction. Applied to the NASA C-MAPSS dataset, the method improves prediction accuracy by 5.5% over existing deep learning approaches while enhancing interpretability and robustness. Authors in [22] propose a method for predicting the RUL of supercapacitors using a Harris Hawks Optimization (HHO) and LSTM neural network. HHO optimizes LSTM parameters to enhance stability and accuracy. Also, in [23] an integrated framework combining data-driven probabilistic RUL prognostics with predictive maintenance planning is introduced.

Power systems are inherently exposed to multiple sources of uncertainty, such as renewable generation intermittency, load demand fluctuations, equipment failures, and market price volatility. Effective modeling of these uncertainties is critical for reliable and economic power system operation and planning. Several approaches have been developed, each suited to different types and levels of uncertainty. Probabilistic methods, such as Monte Carlo Simulation (MCS) and the Point Estimate Method (PEM), rely on historical data to derive probability distribution functions (PDFs) for uncertain parameters. These techniques are widely applied in system planning tasks, including Active Distribution Network Planning (ADNP), to assess the impact of uncertainties through scenario generation. Stochastic Optimization (SO) integrates uncertainty directly into decision-making by generating and solving multiple scenarios. It effectively captures the variability of renewable generation and load demand but can become computationally intensive for large-scale systems. Scenario reduction and clustering methods are commonly used to address this issue. When probability distributions are unavailable or imprecise, possibilistic (fuzzy) approaches offer an alternative by representing uncertain variables with membership functions. Methods such as the α-cut and defuzzification enable analysis under ambiguity, although results are sensitive to the choice of membership functions. RO addresses uncertainty by defining bounded uncertainty sets instead of relying on precise probabilities. This approach seeks solutions that remain feasible under worst-case scenarios, offering practical advantages in real-world applications where data may be limited [24-31].

1.3. Contributions

It is important to note that in prior studies, the GMS problem has generally been addressed without incorporating the RUL of thermal units. However, considering the substantial penalty costs associated with unexpected failures and repairs in thermal power plants, integrating the RUL of generation units is of critical significance. In this paper, the GMS problem is formulated based on the RUL of thermal units and is modeled as a mixed-integer quadratic programming (MIQP) problem. The objective is to minimize the total operating and maintenance costs of the power system over a 52-week planning horizon, while accounting for uncertainties in electrical load demand and renewable energy generation. To this end, the RUL of thermal units is predicted using the LSTM deep learning algorithm, which leverages input data from 21 turbine sensors. Furthermore, a RO approach is employed to address uncertainties associated with electrical load and renewable generation.

The key contributions of this work are as follows:

- Development of a comprehensive RUL-based GMS framework: A novel scheduling model is proposed that integrates RUL into unit commitment decisions, with the aim of reducing system operation and maintenance costs over a one-year (52-week) horizon.
- Introduction of a thermal unit RUL index and its prediction: The RUL of thermal units is quantified and predicted using an LSTM model trained on multivariate time series data obtained from turbine sensors.
- Incorporation of uncertainty in GMS using robust optimization: A RO framework is introduced to ensure reliable scheduling under the worst-case scenarios of load and renewable energy output fluctuations.

1.4. Paper structure

The remainder of this paper is structured as follows: Section 2 presents the mathematical formulation of the RUL-based GMS problem, including the modeling of the RUL prediction using the LSTM network and the integration of uncertainty through a RO framework. Section 3 discusses the case studies and provides a detailed analysis of the simulation results. Finally, Section 4 concludes the paper by summarizing the key findings and contributions.

2. Proposed RUL-based generation maintenance scheduling formulation

This section provides a detailed overview of the RUL-based GMS framework. As illustrated in Fig. 1, the hierarchical structure of the RUL-based GMS incorporates uncertainty considerations. The RUL of generation units is predicted using a deep learning approach, specifically employing a LSTM algorithm applied to time-series data. To address uncertainties in electrical load demand and renewable energy sources (RESs), RO is utilized by formulating a worst-case scenario. In the proposed methodology, the GMS problem is optimized by integrating RUL predictions with the robust modeling of uncertainties, all while adhering to power system constraints. Further details regarding the proposed framework are presented in the subsequent subsections.

2.1. Formulation of proposed RUL-based generation maintenance scheduling problem

The proposed RUL-based GMS formulation is structured as a single-objective optimization problem, aiming to determine the optimal maintenance schedule for generation units while minimizing the total system cost. The objective function comprises two components:

$$Min\left(\sum_{t=1}^{T}\sum_{i=1}^{I}OC_{i,t}+MBPC_{i,t}\right) \quad (1)$$

The first component represents the operating cost of the generation units, modeled as a quadratic function of each unit's power output.

$$OC_{i,t}=\alpha_i\times(P_{i,t})^2+b_i\times P_{i,t}+c_i \quad (2)$$

The second component of objective function corresponds to the Maintenance Breach Penalty Cost (MBPC), which is defined based on the RUL of the units and their full construction cost. The MBPC is formulated exponentially, such that the penalty cost increases at an accelerating rate as the RUL declines, reaching very high values near the end of the unit's lifetime. This formulation ensures that units approaching failure are prioritized for maintenance, thereby avoiding costly reconstructions or unexpected outages. Accordingly, the MBPC acts as an economic mechanism that links technical conditions (RUL) with financial consequences (replacement cost), steering maintenance scheduling toward the simultaneous optimization of reliability and economic efficiency.

$$MBPC_{i,t}=\gamma_i\times e^{\left(h_i\times RUL_{i,t}\right)}\times\left(1-IM_{i,t}\right) \quad (3)$$

In (3), the variable $IM_{i,t}$ is a binary indicator, where a value of 1 signifies that unit i has been repaired on or before time period t, while a value of 0 indicates that the unit has not been repaired or maintained during time period t. The economic objective function presented in (1) is subject to the following set of constraints:

$$\sum_{i=1}^{N}P_{i,t}=L_t-P_t^{PV} \quad (4)$$

$$P_i^{Min}\le P_{i,t}\le P_i^{Max} \quad (5)$$

$$\sum_{t=1}^{T}Z_{i,t}=\omega_i \quad (6)$$

$$\sum_{t=1}^{T}\varpi_{i,t}=1 \quad (7)$$

$$Z_{i,t}-Z_{i,t-1}\le\varpi_{i,t} \quad (8)$$

$$Z_{i,t}+U_{i,t}\le 1 \quad (9)$$

$$IM_{i,t}=Z_{i,t}+IM_{i,t}-q_{i,t} \quad (10)$$

Constraint (4) ensures power balance within the system. The maximum and minimum limitations is enforced on the power output of each generation unit by (5). Constraint (6) pertains to the maintenance duration, where the binary variable $Z_{i,t}$ denotes the maintenance status of each unit—taking a value of 1 if the unit is under maintenance at time t, and 0 otherwise. The one-time maintenance condition is imposed by (7), where the binary variable $\varpi_{i,t}$ indicates

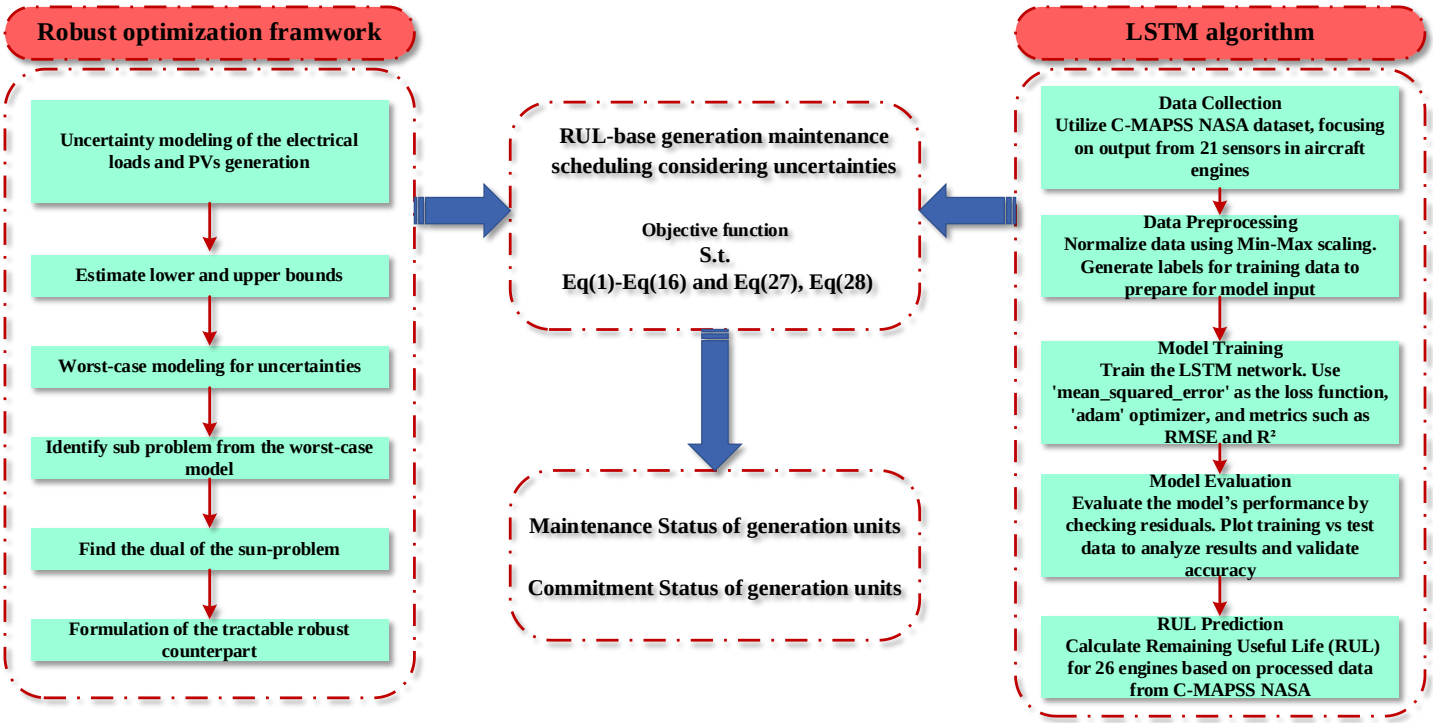

Fig. 1. hierarchical structure of the RUL-based GMS

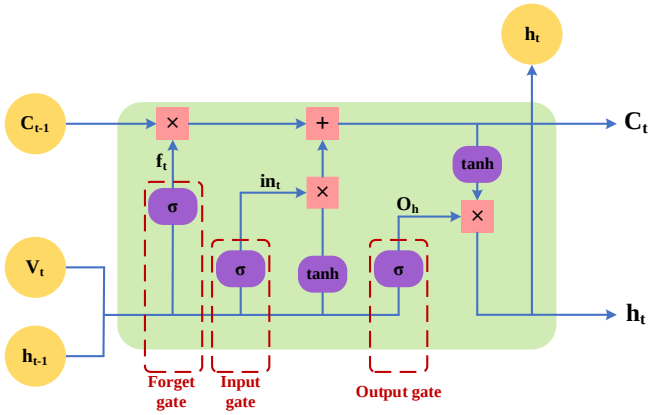

Fig. 2. LSTM architecture

the initiation of maintenance; it is equal to 1 if maintenance begins at the start of time period t , and 0 otherwise. Constraints (8) and (9) represent the maintenance continuity requirement and the link between maintenance status and operational state, respectively. In (9), the binary variable $U_{i,t}$ denotes the commitment status of the unit, taking the value 1 if the unit is operational and 0 if it is offline for any reason [32]. Finally, Constraint (10) updates the variable $IM_{i,t}$ using a binary auxiliary variable to reflect the cumulative maintenance status of each unit.

2.2. RUL Prediction Formulation Using the LSTM Algorithm

In this study, a deep learning approach was employed to predict the RUL of generation units. Deep learning, a subset of machine learning and artificial intelligence, is inspired by the learning processes of the human brain. It plays a crucial role in data science, particularly in areas involving statistical analysis and predictive modeling. Furthermore, deep learning techniques are highly effective in processing and extracting insights from large-scale datasets, making them well-suited for applications involving complex and high-dimensional data such as condition monitoring in power systems [33].

Among the various machine learning and deep learning techniques, LSTM networks have proven to be particularly effective for RUL prediction, owing to their capability to capture long-term dependencies and temporal patterns within sequential data [34]. Recurrent Neural Networks (RNNs) face challenges in capturing long-term dependencies within sequential data due to issues such as vanishing and exploding gradients. To address these limitations, the LSTM network was developed as an enhanced variant of the standard RNN. LSTM networks mitigate gradient-related problems by incorporating a specialized hidden layer known as the memory unit. Each LSTM cell contains three distinct gates that regulate the flow of information. Fig. 2 illustrates the architecture of a typical LSTM unit. The cell state in a LSTM function analogously to a conveyor belt, transferring information along the sequence from time step t−1 to t. Data selection within the LSTM is controlled by gating mechanisms, beginning with the forget gate, which determines the extent to which the current cell state should be retained or discarded. The forget gate is mathematically represented as follows [35]:

$$f_{t,n} = \sigma\left(\sum_j W^{f}_{n,j} h_{t-1,j} + \sum_j U^{f}_{n,j} v_{t,j} + b^{f}_{i}\right) \qquad (11)$$

The input gate constitutes the second component of the LSTM unit and determines the extent to which new information from the input data is allowed to influence the cell state. It can be expressed as follows:

$$in_{t,n} = \sigma\left(\sum_j W^{in}_{n,j} h_{t-1,j} + \sum_j U^{in}_{n,j} v_{t,j} + b^{in}_{i}\right) \qquad (12)$$

The value of the input gate is determined by both the current input signal and the hidden state output from the previous time step. Additionally, the LSTM cell generates new candidate cell memories, which are computed as follows:

$$S_{t+1,n} = f_{t,n} \times S_{t,n} + in_{t,n} \times C_{t,n} \qquad (13)$$

Where:

$$C_{t,n} = \tanh\left(\sum_j W^{C}_{n,j} h_{t-1,j} + \sum_j U^{C}_{n,j} v_{t,j} + b^{C}_{i}\right) \qquad (14)$$

The output gate is the final gating component in the LSTM architecture, responsible for regulating the amount of information from the cell state that is exposed as the output signal. It is mathematically represented by the following equation:

$$O_{t,n} = \sigma\left(\sum_j W^{O}_{n,j} h_{t-1,j} + \sum_j U^{O}_{n,j} v_{t,j} + b^{O}_{i}\right) \qquad (15)$$

Finally, the output of the LSTM cell at the current time step is computed as follows:

$$h_{t,n} = O_{t,n} \times \tanh(S_{t,n}) \qquad (16)$$

The prediction model constitutes another essential component of the framework [36]. One widely used architecture for this purpose is the sequence-to-sequence model, also referred to as the encoder–decoder model. A more detailed explanation of this methodology can be found in [35].

2.3. Uncertainty modeling of electrical loads and PVs output power by RO

RO was first introduced by Soyster in 1970. To enhance the practicality of this approach, authors in [37] developed the concept of adjustable RO. Despite these advancements, the RO framework remained computationally complex. This challenge was later addressed in [38], which introduced the concept of a budget of uncertainty—a tunable parameter determined by the decision maker to balance solution robustness. This paper addresses the uncertainties associated with electrical load demand and PVs panel output using the above Robust approach.

$$\tilde{L}_t = L_t + \Delta L_t \;\; ; \;\; \underline{L}_t \le \Delta L_t \le \vec{L}_t \qquad (17)$$

$$\tilde{P}^{PV}_t = P^{PV}_t + \Delta P^{PV}_t \;\; ; \;\; \underline{P}^{PV}_t \le \Delta P^{PV}_t \le \vec{P}^{PV}_t \qquad (18)$$

The variable bounds for load demand and PV output power are defined in (17) and (18). The uncertainty associated with both load and PV generation is modeled within specified lower and upper bounds, allowing each variable to fluctuate within these limits.

$$\sum_{i=1}^{N} P_{i,t} + P^{UF}_t = L_t + P^{PV}_t \qquad (19)$$

$$P^{UF}_t = Max \left\{ \begin{array}{l} \left(\underline{L}_t \times \underline{r}^{L}_t + \vec{L}_t \times \vec{r}^{L}_t\right) \\ -\left(\underline{P}^{PV}_t \times \underline{r}^{PV}_t + \vec{P}^{PV}_t \times \vec{r}^{PV}_t\right) \end{array} \right\} \qquad (20)$$

The power balance constraint must be satisfied under the worst-case realization of uncertainties. Specifically, the worst-case scenario occurs when the electrical load reaches its maximum value while the output from PVs, is at its minimum. Equation (19) represents the worst-case formulation of the power balance constraint, while (20) defines the corresponding total uncertainty factor (P^{UF}_t).

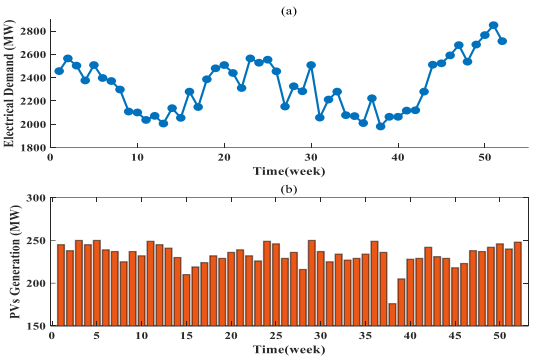

Fig. 3. Weekly profiles (a) Electrical load demand (b) PVs Generation

$$\left\{\left(\vec{r}_t^{\,L}+\vec{r}_t^{\,L}\right)+\left(\vec{r}_t^{\,PV}+\vec{r}_t^{\,PV}\right)\right\}\le\Gamma_t \tag{21}$$

$$0\le\vec{r}_t^{\,L},\vec{r}_t^{\,L},\vec{r}_t^{\,PV},\vec{r}_t^{\,PV}\le 1 \tag{22}$$

The sub-problem within the RO framework, which accounts for uncertainties in load demand and PVs generation, is formulated by taking (19) as the objective function and (21) and (22) as the associated constraints. The dual formulation of this sub-problem is presented in (23) through (26).

$$Min\left\{\zeta_t\times\Gamma_t+\left(\vec{\lambda}_t^{\,L}+\vec{\lambda}_t^{\,L}\right)+\left(\vec{\lambda}_t^{\,PV}+\vec{\lambda}_t^{\,PV}\right)\right\} \tag{23}$$

$$\zeta_t+\vec{\lambda}_t^{\,L}\ge\vec{L}_t\ ;\ \zeta_t+\vec{\lambda}_t^{\,L}\ge\vec{L} \tag{24}$$

$$\zeta_t+\vec{\lambda}_t^{\,PV}\ge\vec{P}_t^{\,PV}\ ;\ \zeta_t+\vec{\lambda}_t^{\,PV}\ge\vec{P}_t^{\,PV} \tag{25}$$

$$\zeta_t,\vec{\lambda}_t^{\,L},\vec{\lambda}_t^{\,L},\vec{\lambda}_t^{\,PV},\vec{\lambda}_t^{\,PV}\ge 0 \tag{26}$$

The tractable robust counterpart formulations for uncertainties in load demand and PVs generation are presented in (27) and (28), respectively. These formulations are derived using the dual problem approach in conjunction with the power balance condition defined in (19).

$$\sum_{i=1}^{N}P_{i,t}+P_t^{\,DU}=L_t+P_t^{\,PV} \tag{27}$$

$$P_t^{\,DU}=\zeta_t\times\Gamma_t+\left(\vec{\lambda}_t^{\,L}+\vec{\lambda}_t^{\,L}\right)+\left(\vec{\lambda}_t^{\,PV}+\vec{\lambda}_t^{\,PV}\right) \tag{28}$$

As RO problems grow in size, computational challenges increase. Larger dimensions add variables and constraints, raising complexity, memory demands, and convergence time. Solvers are more prone to suboptimal solutions, and interpreting or debugging results becomes increasingly difficult.

3. Simulation and numerical results

3.1. Specification of test system

The proposed framework for RUL-based GMS problem has been implemented on modified IEEE-RTS over a scheduling horizon of 52 weeks. The system consists of 26 thermal generation units (N_1-N_{26}), and their corresponding technical specifications are provided in Table 1, as detailed in [39]. Fig. 3 illustrates the weekly profiles of PVs generation and electrical load demand [40]. The dataset utilized for RUL prediction comprises multiple multivariate time series .The input dataset used in this study is the Turbofan Engine Degradation Simulation dataset, developed by the Prognostics Center of Excellence (PCoE) at NASA Ames Research Center [41]. The dataset was generated using the Commercial Modular Aero-Propulsion System Simulation (C-MPASS) framework. It captures engine degradation behavior under varying operational conditions, sensor readings, failure symptoms, and environmental influences, thus including realistic noise and disturbances. Table 2 provide detailed descriptions of symbols and sensor signals used in the turbofan engine degradation dataset. These sensors capture a range of parameters, such as temperature, pressure, compressor and turbine speeds, fuel-to-air ratio, and cooling flow rates.

Table 1. Generating unit information of modified IEEE-RTS

Unit	P_i^{Min} / P_i^{Max} (MW)	ω_i (week)	α_i	b_i	c_i	γ_i (M$)	h_i
1	100/400	5	0.00195	7.503	311.910	200	-0.112000896
2	140/350	4	0.00153	10.862	177.058	175	-0.098000784
3	68.95/197	3	0.00263	23.200	260.176	98.5	-0.05516044128
4	54.25/155	3	0.00487	10.758	143.597	77.5	-0.0434003472
5	54.25/155	3	0.00481	10.737	143.318	77.5	-0.0434003472
6	25/100	2	0.00598	18.200	218.775	50	-0.028000224
7	25/100	2	0.00612	18.100	218.335	50	-0.028000224
8	15.2/76	2	0.00932	13.407	81.626	36	-0.0201601628
9	15.2/76	2	0.00910	13.381	81.464	36	-0.0201601628
10	4/20	1	0.01433	37.890	118.821	10	-0.0056000448
11	4/20	1	0.01359	37.777	118.458	10	-0.0056000448
12	2.4/12	1	0.02855	24.888	24.888	6	-0.003360002688
13	2.4/12	1	0.02842	24.761	24.761	6	-0.003360002688
14	2.4/12	1	0.02801	24.638	24.638	6	-0.003360002688
15	100/400	5	0.00194	7.492	310.000	200	-0.112000896
16	68.95/197	3	0.00260	23.100	259.131	98.5	-0.05516044128
17	68.95/197	3	0.00259	23.000	259.131	98.5	-0.05516044128
18	54.25/155	3	0.00473	10.715	143.029	77.5	-0.0434003472
19	54.25/155	3	0.00463	10.694	142.735	77.5	-0.0434003472
20	25/100	2	0.00623	18.000	217.895	50	-0.028000224
21	15.2/76	2	0.00895	13.354	81.298	36	-0.0201601628
22	15.2/76	2	0.00876	13.327	81.136	36	-0.0201601628
23	4/20	1	0.01261	37.664	118.108	10	-0.0056000448
24	4/20	1	0.01191	37.551	117.755	10	-0.0056000448
25	2.4/12	1	0.02649	25.675	24.411	6	-0.003360002688
26	2.4/12	1	0.02533	25.547	24.389	6	-0.003360002688

Table 2. Symbols and description of sensor signals for turbofan engine degradation dataset

NO.	Symbol	description	Units
1	*T2*	Total temperature at fan inlet	*°R*
2	*T24*	Total temperature at LPC outlet	*°R*
3	*T30*	Total temperature at HPC outlet	*°R*
4	*T50*	Total temperature at LPT outlet	*°R*
5	*P2*	Pressure at fan inlet	*psia*
6	*P15*	Total pressure in bypass duct	*psia*
7	*P30*	Total pressure at HPC outlet	*psia*
8	*Nf*	Physical fan speed	*rpm*
9	*Nc*	Physical core speed	*rpm*
10	*Epr*	Engine Pressure ratio	-
11	*Ps30*	Static pressure at HPC outlet	*psia*
12	*Phi*	Ratio of fuel flow to Ps30	*pps/psi*
13	*NRF*	Corrected fan speed	*rpm*
14	*NRc*	Corrected core speed	*rpm*
15	*BPR*	Bypass ratio	-
16	*farB*	Burner fuel-air ratio	-
17	*htBleed*	Bleed enthalpy	-
18	*Nf_dmd*	Demanded fan speed	*rpm*
19	*PCNfR_dmd*	Demanded corrected fan speed	*rpm*
20	*W31*	HPT coolant bleed	*lpm/s*
21	*W32*	LPT coolant bleed	*lpm/s*

In this paper the uncertainty budget (Γ_t) is set to 0.2, and the optimization problem is solved using the Cplex solver within the GAMS software environment.

3.2. Case studies

To evaluate the effectiveness of the proposed framework, three case studies have been defined as follows:

- **Case I**: Robust GMS without incorporating the RUL prediction
- **Case II**: Robust GMS based on RUL prediction

3.3. Simulation results

Accurate prediction of RUL is essential for minimizing maintenance and repair costs, preventing unexpected outages, optimizing resource allocation, and extending the operational lifespan of equipment. In this study, an LSTM neural network is trained using input features extracted from 21 turbine sensors for each generation unit. The trained model is then used to predict the RUL of each thermal unit over a one-year horizon.

Fig. 4 illustrates the RUL values of 26 thermal units during the first week. In this figure, the RUL value represents the estimated time remaining before a unit reaches the end of its functional life. For instance, the fourth unit is projected to fail in approximately 60 weeks, indicating that it will require significant repairs or a complete overhaul at that point. Table 3 presents the maintenance status and maintenance intervals of the units under two case studies. In Case I, the GMS is optimized without incorporating RUL of the units, and as such, no economic penalties are imposed for maintenance breach. Conversely, in Case II, the GMS is optimized with consideration of the RUL, and the associated penalty costs for maintenance breach are included in the objective function. This approach enables a more comprehensive optimization, whereby both operating costs and maintenance-related expenses are minimized, leading to improved reliability and cost-effectiveness of the scheduling strategy. Fig. 5a and Fig. 5b illustrates the power generation of thermal units during weeks #9 and #41, respectively. In week #9, the electrical demand is met by thermal units N_1, N_2, N_4, N_5, N_8, N_9, N_{15}, N_{18}, N_{19}, N_{21}, and N_{22}. In Case I, where GMS is performed without considering the RUL, unit N_8 is offline with no production, and unit N_{22} is undergoing maintenance. Consequently, the demand is met by the remaining active units, including unit N_{19}. In contrast, in Case II, where GMS is based on the RUL index, unit N_{19} is scheduled for maintenance in week #9—identified as the optimal maintenance window based on its RUL prediction. Therefore, units N_8 and N_{22} remain operational to compensate for the absence of unit N_{19}, thereby avoiding potential penalty costs associated with delayed maintenance.

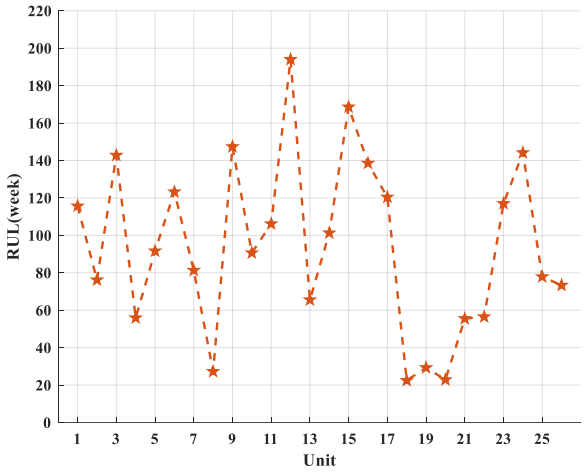

Fig. 4. RUL Values of 26 Thermal Units in the First Week

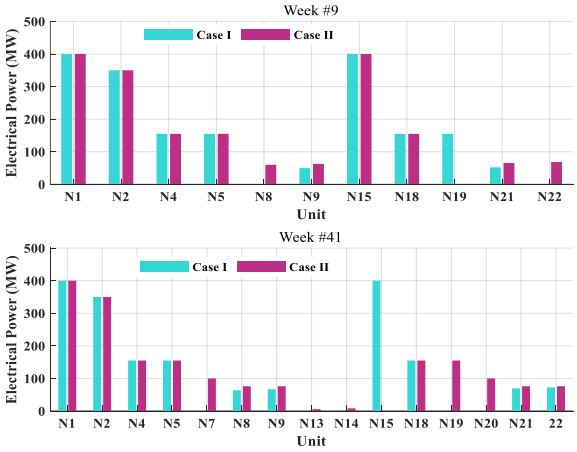

Fig. 5. Power generation of thermal units. (a) Week #9. (b) Week #41

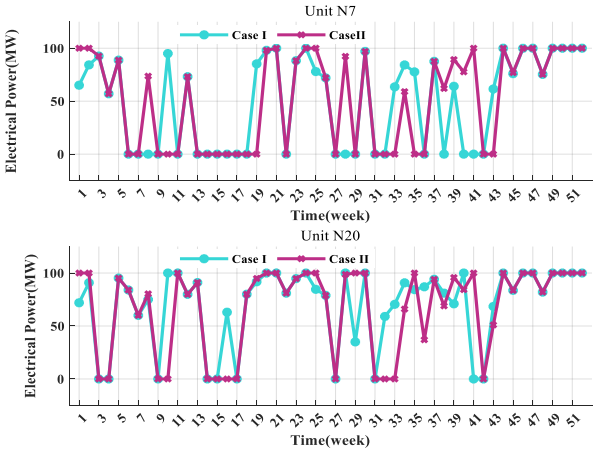

Fig. 6. Annual power generation profiles of thermal units. (a) Unit N_7. (b) Unit N_{20}.

Table 3. Maintenance status of 26 units

Unit	N1	N2	N3	N4	N5	N6
Case1	34-36	37-40	50-52	27	31-33	18-19
Case2	11-13	34-37	50-52	17	27-29	25-26
Unit	N7	N8	N9	N10	N11	N12
Case1	6-7	28-29	21-22	47	26	48
Case2	18-19	1-2	42-43	5	7	33
Unit	N13	N14	N15	N16	N17	N18
Case1	5	49	10-13	23-25	44-46	14-15
Case2	16	30	38-41	47-49	44-46	14-15
Unit	N19	N20	N21	N22	N23	N24
Case1	41-43	3-4	16-17	8-9	30	2
Case2	8-10	3-4	21-22	31-32	6	23
Unit	N25	N26				
Case1	20	1				
Case2	24	20				

In week #41, the electrical load is supplied by thermal units N_1, N_2, N_4, N_5, N_7–N_9, N_{13}–N_{15}, and N_{18}–N_{22}, as shown in Fig. 5b. In Case I, unit N_{19} is scheduled for maintenance, and the demand is balanced by the remaining units, including unit N_{15}. However, in Case II, the RUL-based GMS approach identifies week #41 as the optimal time for the maintenance of unit N_{15}. As a result, unit N_{15} is taken offline for maintenance, and units N_7, N_{13}, N_{14}, N_{19}, and N_{20} are brought online to maintain system balance. The total generation in week #41 amounts to 1888 MW, ensuring the demand is fully met under both scheduling strategies.

Table 4. Thermal units' commitment status in case I

Unit	Decommitted	Committed
N1	34-36	1-33,37-52
N2	37-40	1-36,41-52
N3	1-52	-
N4	-	1-52
N5	31-33	1-30,34-52
N6	1,4-22,24,26-36,38-44	2-3,5-21,23,25,37,45-52
N7	6-9,13-18,22,27-29,31-32,36,38,40-42	1-5,10-12,19-21,23-26,30,33-35,37,39,43-52
N8	9,17,28-29,31,34-36	1-8,10-16,18-27,30,32-33,37-52
N9	21-22	1-20,23-52
N10	-	1-52
N11	-	1-52
N12	1-50,52	51
N13	1-50,52	51
N14	1-10,12-16,18-20,22-23,25-27,29-39,41-43,45-50,52	11,17,21,24,28,40,44,51
N15	10-13	1-9,14-52
N16	1-52	-
N17	1-46,48	47,49-52
N18	14-15	1-14,16-52
N19	41-43	1-40,44-52
N20	3-4,14-15,17,31,41-42	1-2,5-13,16,18-30,32-40,43-52
N21	16-17	1-15,18-52
N22	8-9	1-7,10-52
N23	1-52	-
N24	1-52	-
N25	1-52	-
N26	1-50,52	51

Fig. 6a and Fig. 6b depicts the annual power generation profiles of thermal units N_7 and N_{20}, respectively. For unit N_7, in Case I—where the GMS is performed without considering the RUL—maintenance and repair activities are scheduled during weeks #6 and #7. The total annual energy production of this unit amounts to 2564 MW. Over the 52-week horizon, unit N_7 remains offline for 22 weeks and contributes to power generation during the remaining 30 weeks. In Case II, where GMS is optimized based on RUL, maintenance for unit N_7 is scheduled in weeks #18 and #19. This results in a slightly higher total generation of 2660.56 MW, with the unit still offline for 22 weeks, indicating improved scheduling efficiency based on the unit's degradation status.

Table 5. Thermal units' commitment status in case II

Unit	Decommitted	Committed
N1	11-13	1-10,14-52
N2	34-37	1-33,38-52
N3	1-52	-
N4	17	1-16,18-52
N5	27-29	1-26,30-52
N6	1,4-18,20-36,38-44	2-3,19,37,45-52
N7	6-7,9-11,13-19,22,27,29,31-33,35-36,42-43,	1-5,8,12,20-21,23-26,28,30,34,37-41,44-52
N8	1-2	3-52
N9	31,42-43	1-30,32-41,44-52
N10	1-52	-
N11	1-52	-
N12	1,3-24,26-50,52	2,25,51
N13	3-10,12-24,26-28,30-40,42-50,52	1-2,11,25,29,41,51
N14	3-10,12-16,18-20,22-23,26-28,30-34,36-40,42-43,45-50,52	1-2,11,17,21,24-25,29,35,41,44,51
N15	38-41	1-37,42-52
N16	1-52	-
N17	1-46,48	47,49-52
N18	14-15	1-13,16-52
N19	8-10	1-7,11-52
N20	3-4,14-17,27,31-33,42	1-2,5-13,18-26,28-30,34-41,43-52
N21	21-22	1-20,23-52
N22	31-32	1-30,33-52
N23	1-52	-
N24	1-52	-
N25	1-52	-
N26	1-50,52	51

Table 6. Costs comparison of case studies.

Cases	Operation Cost ($)	Maintenance Cost ($)	Total Cost ($)
I	1,328,669.403	36,369.005	1,365,038.408
II	1,329,337	2,750.92	1,332,088.918

Fig. 6b illustrates the power generation of unit N_{20}. In Case I, maintenance is conducted during weeks #3 and #4, and the unit generates a total of 3698 MW annually, remaining offline for 10 weeks throughout the year. In Case II, the maintenance schedule remains the same; however, the total annual generation is reduced to 3481.26 MW. This decrease is attributed to the optimized GMS based on RUL, which may have limited the unit's operation during periods of critical degradation to prevent failure. Consequently, in Case II, unit N_{20} operates for 39 weeks and is offline for 13 weeks, demonstrating how RUL-based scheduling can influence operational patterns to enhance system reliability and reduce potential failure costs. The detailed commitment status of the thermal units under the first two studied cases is presented in Table 4 and Table 5, respectively.

Table 6 presents a comparative analysis of operation and maintenance costs across the two defined case studies. In the first scenario, where the maintenance schedule is determined solely by

classical constraints without considering the predicted remaining useful life (RUL), total operating costs are slightly lower since units remain in service for longer durations. However, this approach overlooks actual wear conditions, causing maintenance to be delayed and ultimately leading to significantly higher maintenance costs. As a result, the overall cost, including both operation and maintenance, is higher than in the second scenario. In contrast, the second scenario incorporates accurate RUL predictions obtained from the LSTM model to adjust the maintenance schedule. While this leads to a slight increase in operating costs—since some units are removed earlier and load redistribution is required—it substantially reduces maintenance costs by servicing units before reaching critical conditions and avoiding costly failures. Consequently, the total system cost decreases, achieving a net reduction of 2.41% compared to the first scenario.

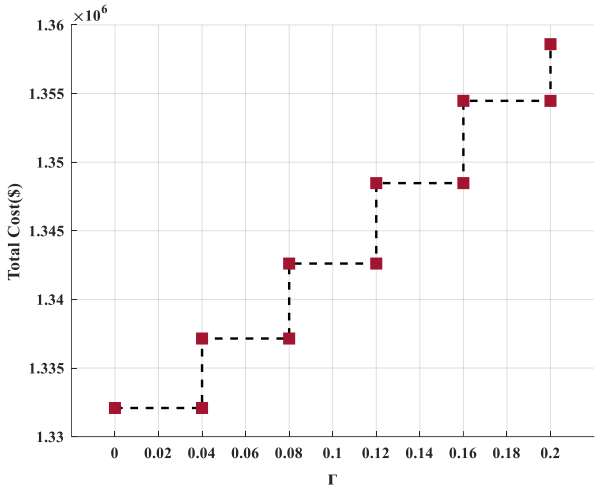

Fig. 7. Sensitivity analysis on Γ_t.

However, incorporating a RO approach to account for uncertainties in electrical load and renewable energy production can increase total costs depending on the level of robustness employed.

Fig. 7 illustrates the impact of varying the robustness level, denoted by the parameter Γ_t, on total system costs. As the value of Γ_t increases, the scaled deviations of both load ($\hat{r}_t^L$, $\check{r}_t^L$) and PVs generation ($\hat{r}_t^{PV}$, $\check{r}_t^{PV}$) become more pronounced. This intensifies the mismatch between load demand and PVs output—manifested as higher demand and lower PVs generation—thereby increasing uncertainty and creating a more adverse operating scenario. Consequently, the system must rely more heavily on thermal units, leading to higher system's total cost.

4. Conclusion

In this paper, a novel approach for GMS is proposed based on the RUL of thermal units. The main objective is to minimize the overall system operation and maintenance costs. Additionally, a RO framework is incorporated to address the uncertainties associated with electrical loads and PVs generation. The proposed model is implemented on a modified IEEE-RTS, which includes 26 thermal generation units as well as PV resources. To assess the effectiveness of the RUL-based GMS, two case studies are conducted. The results demonstrate that while the RUL-based scheduling may increase operational costs in certain weeks, it achieves a reduction of 7.56% in maintenance costs over the one-year planning horizon. Furthermore, the RO framework effectively mitigates the impact of uncertainties in demand and renewable generation, with a marginal cost increase of up to 2%, depending on the selected robustness level. The effectiveness of the proposed RUL-based GMS critically depends on the availability and quality of operational and condition-monitoring data from thermal units. Accurate estimation of RUL necessitates comprehensive historical and real-time information on equipment degradation, maintenance records, and operational conditions. Future research can enhance the RUL-based GMS framework by integrating demand response, energy storage, and flexible generation to better manage uncertainties in demand and renewables. Additionally, studying grid resiliency under high-impact, low-probability events can improve reliability and maintenance planning, resulting in a more robust framework for modern power systems.

Reference

[1] L. Moyo, N. I. Nwulu, U. E. Ekpenyong, and R. C. Bansal, "A Tri-Objective model for generator maintenance scheduling," *IEEE Access*, vol. 9, pp. 136384–136394, Jan. 2021.

[2] J. Caboz. (Mar. 18, 2019). Business Insider South Africa. Accessed: Jun. 29, 2019. [Online]. Available: https://www.businessinsider.co.za/6-quick-fixes-that-can-save-south-africa-from-more-load-shedding-2019-3.

[3] Eskom. (May 18, 2019). Interpreting Scedules. Eskom. Accessed: Jun. 29, 2019. [Online]. Available: http://loadshedding.eskom.co.za/LoadShedding/ScheduleInterpretation.

[4] A. Hassanpour and E. Roghanian, "A two-stage stochastic programming approach for non-cooperative generation maintenance scheduling model design," International Journal of Electrical Power & Energy Systems, vol. 126, p. 106584, Oct. 2020.

[5] V. Sharifi, A. Abdollahi, and M. Rashidinejad, "Flexibility-based generation maintenance scheduling in presence of uncertain wind power plants forecasted by deep learning considering demand response programs portfolio," *International Journal of Electrical Power & Energy Systems*, vol. 141, p. 108225, Apr. 2022.

[6] S. Amiri, M. Honarvar, and A. Sadegheih, "Providing an integrated Model for Planning and Scheduling Energy Hubs and preventive maintenance," *Energy*, vol. 163, pp. 1093–1114, Aug. 2018.

[7] M. Javidsharifi, T. Niknam, J. Aghaei, and G. Mokryani, "Multi-objective short-term scheduling of a renewable-based microgrid in the presence of tidal resources and storage devices," *Applied Energy*, vol. 216, pp. 367–381, Feb. 2018.

[8] N. Lee, J. Woo, and S. Kim, "A deep reinforcement learning ensemble for maintenance scheduling in offshore wind farms," *Applied Energy*, vol. 377, Art. 124431, 2025.

[9] P. Prukpanit, P. Kaewprapha, and N. Leeprechanon, "Optimizing generation maintenance scheduling considering emission factors," *Energies*, vol. 16, no. 23, p. 7775, Nov. 2023.

[10] X. An, G. Si, T. Xia, D. Wang, E. Pan, and L. Xi, "An energy-efficient collaborative strategy of maintenance planning and production scheduling for serial-parallel systems under time-of-use tariffs," *Applied Energy*, vol. 336, p. 120794, Feb. 2023.

[11] X. Zhang, X. Wu, B. Cao, X. Wang, and B. Wang, "An efficient generator maintenance scheduling model based on unit clustering and linear relaxation," *Electric Power Systems Research*, vol. 230, p. 110300, Mar. 2024.

[12] V. F. Yu, Q. V. N. Truc, and N. N. Minh, "Integrated maintenance scheduling for generators and transmission lines considering renewable energy sources and energy storages," *Electric Power Systems Research*, vol. 246, p. 111696, Apr. 2025.

[13] L. Liu, Y. Xiao, and J. Yang, "Daily optimization of maintenance routing and scheduling in a large-scale photovoltaic power plant with time-varying output power," *Applied Energy*, vol. 360, p. 122793, Feb. 2024.

[14] S. Salarkheili, M. S. Nazar, D. Wozabal, and F. Jabari, "Capacity

withholding of GenCos in electricity markets using security-constrained generation maintenance scheduling," *International Journal of Electrical Power & Energy Systems*, vol. 146, p. 108771, Nov. 2022.

[15] S. B. Kivade, N. I. Jamadar, "Prediction of Remaining useful life of Mechanical Components – A Review," *International Journal of Engineering Education,* Vol. 2, p. 1-5, Oct. 2014.

[16] C. Okoh, R. Roy, J. Mehnen, and L. Redding, "Overview of remaining useful life prediction techniques in through-life engineering services," *Procedia CIRP*, vol. 16, pp. 158–163, Jan. 2014.

[17] Y. Wang, Y. Zhao, and S. Addepalli, "Remaining Useful Life Prediction using Deep Learning Approaches: A Review," *Procedia Manufacturing*, vol. 49, pp. 81–88, Jan. 2020.

[18] D. She and M. Jia, "A BiGRU method for remaining useful life prediction of machinery," *Measurement*, vol. 167, p. 108277, Jul. 2020.

[19] J. Liang, H. Liu, and N.-C. Xiao, "A hybrid approach based on deep neural network and double exponential model for remaining useful life prediction," *Expert Systems with Applications*, vol. 249, Art. 123563, 2024.

[20] X. Li, D. Yu, V. S. Byg, and S. D. Ioan, "The development of machine learning-based remaining useful life prediction for lithium-ion batteries," *Journal of Energy Chemistry*, vol. 82, pp. 103–121, Apr. 2023.

[21] Y. Li, Y. Chen, Z. Hu, and H. Zhang, "Remaining useful life prediction of aero-engine enabled by fusing knowledge and deep learning models," *Reliability Engineering & System Safety*, vol. 229, p. 108869, Oct. 2022.

[22] N. Ma, H. Yin, and K. Wang, "Prediction of the remaining useful life of supercapacitors at different temperatures based on improved Long Short-Term memory," *Energies*, vol. 16, no. 14, p. 5240, Jul. 2023.

[23] J. Lee and M. Mitici, "Deep reinforcement learning for predictive aircraft maintenance using probabilistic Remaining-Useful-Life prognostics," *Reliability Engineering & System Safety*, vol. 230, p. 108908, Oct. 2022.

[24] Z. Hao, F. Di Maio, and E. Zio, "Monte Carlo Tree Search-based Deep Reinforcement Learning for Flexible Operation & Maintenance Optimization of a Nuclear Power Plant," *Journal of Safety and Sustainability*, vol. 1, no. 1, pp. 4–13, Sep. 2023.

[25] S. Poorvaezi Roukerd, A. Abdollahi, M. Rashidinejad, "Uncertainty-based unit commitment and construction in the presence of fast ramp units and energy storages as flexible resources considering enigmatic demand elasticity," *Journal of Energy Storage*, vol. 29, Art. 101290, 2020.

[26] N. Randall and B. Basciftci, "Risk-averse contextual predictive maintenance and operations scheduling with flexible generation under wind energy uncertainty," *European Journal of Operational Research*, vol. 327, no. 1, Art. 06 005, June 2025.

[27] Z. Zhong, N. Fan, and L. Wu, "Multistage Stochastic optimization for mid-term integrated generation and maintenance scheduling of cascaded hydroelectric system with renewable energy uncertainty," *European Journal of Operational Research*, vol. 318, no. 1, pp. 179–199, May 2024.

[28] D. Mirzaei, A. Behbahaninia, A. Abdalisousan, and S. M. M. Lavasani, "A novel approach to repair time prediction and availability assessment of the equipment in power generation systems using fuzzy logic and Monte Carlo simulation," *Energy*, vol. 282, p. 128842, Aug. 2023.

[29] M. A. Moghadam, S. Bagheri, A. H. Salemi, and M. B. Tavakoli, "Long-term and multi-objective maintenance scheduling of medium voltage overhead lines based on LP metric method," *IET Generation Transmission & Distribution*, vol. 18, no. 7, pp. 1478–1493, Feb. 2024.

[30] M. Rahmani-Andebili, A. Abdollahi, and M. P. Moghaddam, "An investigation of implementing Emergency Demand Response Program (EDRP) in Unit Commitment problem," in *Proc. IEEE Power & Energy Society General Meeting*, San Diego, CA, USA, 2011, pp. 1–7.

[31] S. Salarkheili, M. S. Nazar, D. Wozabal, and F. Jabari, "Capacity withholding of GenCos in electricity markets using security-constrained generation maintenance scheduling," *International Journal of Electrical Power & Energy Systems*, vol. 146, p. 108771, Nov. 2022.

[32] M. Mollahassani-Pour, M. Rashidinejad, A. Abdollahi, and M. A. Forghani, "Demand response Resources' allocation in Security-Constrained Preventive Maintenance Scheduling via MODM method," *IEEE Systems Journal*, vol. 11, no. 2, pp. 1196–1207, Mar. 2016.

[33] G. W. Chang and H.-J. Lu, "Integrating GRAY Data Preprocessor and Deep Belief Network for Day-Ahead PV Power Output Forecast," *IEEE Transactions on Sustainable Energy*, vol. 11, no. 1, pp. 185–194, Dec. 2018.

[34] S. Yousuf, S. A. Khan, and S. Khursheed, "Remaining useful life (RUL) regression using Long–Short Term Memory (LSTM) networks," *Microelectronics Reliability*, vol. 139, p. 114772, Sep. 2022.

[35] L. Zhu, Z. Yan, W.-J. Lee, X. Yang, Y. Fu, and W. Cao, "Direct load control in microgrids to enhance the performance of integrated resources planning," *IEEE Transactions on Industry Applications*, vol. 51, no. 5, pp. 3553–3560, Mar. 2015.

[36] K. Cho et al., "Learning Phrase Representations using RNN Encoder-Decoder for Statistical Machine Translation," arXiv.org, 2014.

[37] A. Ben-Tal, A. Goryashko, E. Guslitzer, and A. Nemirovski, "Adjustable robust solutions of uncertain linear programs," *Mathematical Programming*, vol. 99, no. 2, pp. 351–376, Mar. 2004.

[38] A. Hussain, V.-H. Bui, and H.-M. Kim, "Robust Optimization-Based scheduling of Multi-Microgrids considering uncertainties," *Energies*, vol. 9, no. 4, p. 278, Apr. 2016.

[39] M. Mollahassani-Pour, A. Abdollahi, and M. Rashidinejad, "Investigation of Market-Based Demand Response Impacts on Security-Constrained Preventive Maintenance scheduling," *IEEE Systems Journal*, vol. 9, no. 4, pp. 1496–1506, Jan. 2014.

[40] P. Subcommittee, "IEEE Reliability Test System," *IEEE Transactions on Power Apparatus and Systems*, vol. PAS-98, no. 6, pp. 2047–2054, Nov. 1979.

[41] A. Saxena, K. Goebel, D. Simon, and N. Eklund, "Damage propagation modeling for aircraft engine run-to-failure simulation," *2008 International Conference on Prognostics and Health Management*, Oct. 2008.